Exact enumeration approach to the directed polymer problem

Pierre Devillard and H. Eugene Stanley
Center for Polymer Studies and Department of Physics, Boston University, Boston, Massachusetts 02215
(Received 20 July 1989)

An exact enumeration approach is developed for the directed polymer problem. The probability distribution of the number of directed self-avoiding walks that can reach a certain level t is obtained exactly up to $t=10$. This enables us to calculate some properties of directed polymers that are not attainable by Monte Carlo simulations. Specifically, we find that the fluctuation of the logarithm of the number of directed self-avoiding walks that can reach level t, when averaged over the configurations that can reach level t, scales as $t^{1/2}$ well below the directed percolation threshold p_{cD}, contrary to the behavior $t^{1/3}$, which is known to be valid when the bond probability p is above p_{cD}. When p is close to 1, these fluctuations scale as $t^{1/5}$ for a very long time before the true asymptotic behavior $t^{1/3}$ is recovered. The method can also be used to obtain the behavior of averages of moments of the number of directed self-avoiding walks that can reach level t. Below p_{cD} these quantities are dominated by rare configurations and cannot be obtained by Monte Carlo simulations.

I. INTRODUCTION AND MOTIVATION

The directed polymer (DP) in a random introduced by Nadal and Vannimenus[1] and also by Kardar, Parisi, and Zhang[2,3] has stirred much interest.[4-10] This has also been referred to in the literature as the directed self-avoiding-walk problem (DSAW); we shall use these two terms as equivalent. In the simplest version, for $d=2$, one starts with the square lattice rotated by 45° (Fig. 1). We call t the upward direction and x the transverse direction. It is customary to refer to the upward direction as the "time." We are interested in directed self-avoiding walks, that is, self-avoiding walks (SAW) that start from the origin and are not allowed to go down in the negative t direction. Bonds are present with probability p and absent with probability $1-p$. We are interested in the probability distribution of the number of (DSAW's) that can reach some level t.

For $d=2$, the DSAW is equivalent[6-8] to the roughening of domain walls in a quenched random exchange Ising model. The DSAW can also be related to many other problems such as growth of Eden clusters,[2] large time behavior of randomly stirred fluids,[2,11] and flame fronts.[12]

In general, two techniques have been used. One is Monte Carlo sampling of the configurations followed by exact enumeration of the DSAW's for each configuration.[1,2,6-8] The other is a mapping onto the Bürgers equation (or some equations related to it) that was treated by field-theory renormalization techniques.[2,6-8,11]

Our purpose is twofold. We propose a new approach to the DP based on exact enumerations.

(i) This may be of some use since it can be in principle extended to d larger than 1, where the DSAW problem is very controversial.

(ii) For $d=2$, the probability distribution of the logarithm of the number of DSAW's has long tails.[1] If one wants to calculate averages of moments of the number of DSAW's, one cannot use the log-normal distribution. Our approach can bring some information on those properties, which are governed by rare events and have not been obtained by the other methods mentioned above. We also can obtain information for very small p.

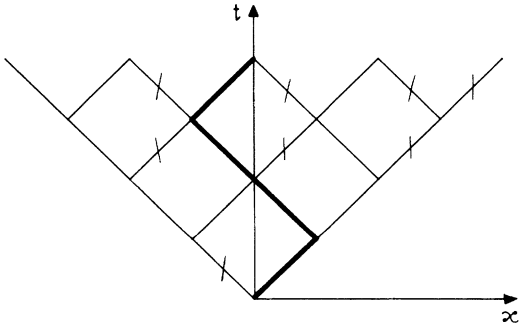

FIG. 1. A particular configuration of the random matrix of size $t=4$. Bonds that have been cut are denoted by a slash. The heavy line denotes a particular DSAW.

II. MODEL

We shall consider here the case $d=2$ (one space plus one time dimension). On the undilute (full) lattice, there are 2^t DSAW's starting from the origin that can reach level t. We treat a dilute lattice with quenched disorder. For each configuration C, $N_C(t)$ is the number of DSAW's starting from the origin O and reaching level t. $N_C(t)$ may be zero. The probability that there are ω DSAW's reaching level t is

$$\Pi(\omega,t)=\sum_C W(C)\delta(N_C(t)-\omega)\ , \tag{1}$$

where the summation is over all the configurations C and $W(C)$ denotes the weight of a configuration. This proba-

 ©1990 The American Physical Society

bility distribution $\Pi(\omega,t)$ depends of course on p, but we omit the index p in order to ease the notation.

Following Ref. 1, we next introduce two auxiliary functions.

(i) The first function is P_t, the probability that there is at least one directed path to level t. Thus, for $\omega=0$,

$$\Pi(0,t)=1-P_t \quad (\omega=0) . \tag{2a}$$

(ii) The second function is $\Delta(\omega,t)$ defined through the relation

$$\Pi(\omega,t)=P_t\Delta(\omega,t) \quad (\omega\neq 0) , \tag{2b}$$

since in order to reach level t, we must have at least one DSAW. Considering (2a) and (2b), we write for arbitrary ω

$$\Pi(\omega,t)=(1-P_t)\delta(\omega)+\sum_{\omega'=1}^{2^t} P_t\Delta(\omega-\omega',t) . \tag{2c}$$

The first moment of $P_t(\omega)$ is simply $\langle N_{\rm SAW}\rangle$, the average number of DSAW's that reaches level t,

$$\langle N_{\rm SAW}\rangle \equiv \int \Pi(\omega,t)\omega\, d\omega . \tag{3a}$$

Since there are at each level two bonds that go to the next level, we expect

$$\langle N_{\rm SAW}\rangle=(2p)^t . \tag{3b}$$

There are three regimes according to whether p is larger or smaller than the directed percolation threshold p_{cD}. The properties of the function P_t are known for each regime.[13]

(i) $p>2_{cD}$. P_t tends to a constant as t tends to infinity.

(ii) $p=p_{cD}$. P_t decays as a power law

$$P_t\sim t^{-\beta/\nu_\parallel} , \tag{4a}$$

where β is the directed percolation probability exponent and $\nu_\parallel$ the parallel correlation length exponent.

(iii) $p<p_{cD}$. We expect exponential decay

$$P_t\sim\exp\left[-\frac{t}{\xi_\parallel}\right] , \tag{4b}$$

where $\xi_\parallel$ is the parallel correlation length.

There are two kinds of configuration averages, averages over only those configurations that span and averages over all configurations. The first kind of average of a quantity Q will be denoted by $\langle Q\rangle_{\rm span}$ and the second kind by $\langle Q\rangle_{\rm all}$. For all nonzero p, it is known that[1]

$$\langle \ln N_{\rm SAW}\rangle_{\rm span}\sim t . \tag{5}$$

The behavior of the fluctuations of the logarithm of DSAW's is also known. Based on the analogy with the Bürgers equation,[6–8] for $p>p_{cD}$, we have

$$F(t)\equiv[\langle(\ln N_{\rm SAW}-\langle \ln N_{\rm SAW}\rangle_{\rm span})^2\rangle_{\rm span}]^{1/2}\sim t^{1/3} . \tag{6}$$

We would like to have some more information about the distribution $\Pi(\omega,t)$. For example, we would like to estimate how its width grows below and at p_{cD}. It has also been shown[1] that the distribution has long Lifschitz tails for large values of ω, but the characteristics of these tails are not attainable by Monte Carlo simulations. Hence we propose using the method of exact enumeration.[14] The principle is to enumerate *all* the different possible configurations (there are $2^{t(t+1)}$ configurations) and for each configuration to count the number of DSAW's that can reach level t. This is equivalent to solving the problem *exactly* for finite t. Then, using extrapolation techniques, we try to guess the asymptotic behavior for large t.

III. COMPUTATION TECHNIQUE

We now describe the method we used to obtain $\Pi(\omega,t)$. Consider a system of size t (see Fig. 1). Since there are $t(t+1)$ bonds that reach level t, P_t is a polynomial of degree $t(t+1)$. A configuration with n occupied bonds must have $t(t+1)-n$ empty bonds and hence a weight

$$W=p^n q^{t(t+1)-n} , \tag{7}$$

where

$$q\equiv 1-p . \tag{8}$$

Thus P_t is in fact a polynomial of degree $t(t+1)$ in the variable p. For fixed t, for any number ω of DSAW's between 1 and 2^t, all the $\Delta(\omega,t)$ are polynomials of order $t(t+1)$ in the variable p. Up to $t=4$, we enumerate all the configurations directly. For $t=5$, we develop a transfer-matrix algorithm (Appendix A).

Due to memory requirements, it is difficult to go beyond $t=5$. We therefore also studied a slightly different problem. Instead of looking at the wedge portion of the square lattice rotated by 45° and limited to time lower than t (Fig. 1), we consider the geometry shown in Fig. 2. Our system is now a diamond whose diagonal along the time direction has length $2t$. We denote by $P_2(t)$ the probability of reaching the uppermost point M at level $2t$. $\Pi_2(\omega,t)$ will denote the probability of having a number ω of DSAW's from O to M. In the limit of large t, the behavior of $P_2(t)$ is expected to be the following:[13] For $p>p_{cD}$, $P_2(t)$ tends to a constant as $t\to\infty$. For $p=p_{cD}$,

$$P_2(t)\sim t^{-2(\beta/\nu_\parallel)} . \tag{9a}$$

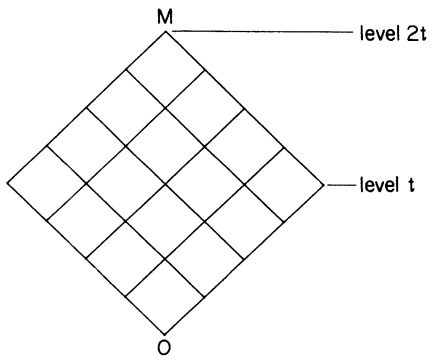

FIG. 2. Diamond-shaped version of the random matrix. M is the uppermost point.

For $p < p_c D$,

$$P_2(t) \sim \exp(-2t/\xi_{\parallel}) . \tag{9b}$$

There are two kinds of configuration average. The average of a quantity Q over all configurations that span from O to M will be denoted by $\langle Q \rangle_{OM}$, whereas the average on all configurations will be denoted by $\langle Q \rangle_{\text{all}}$.

IV. RESULTS

The series up to $t=4$ for the wedge portion of the square lattice are reported in Appendix B. The knowledge of $\Pi_2(\omega,t)$ enables us to calculate P_{2t}, $\langle \ln N_{\text{SAW}} \rangle_{OM}$, and the fluctuations

$$F_2(t) \equiv (\langle (\ln N_{\text{SAW}} - \langle \ln N_{\text{SAW}} \rangle_{OM})^2 \rangle_{OM})^{1/2} , \tag{10}$$

where $F_2(t)$ is defined in analogy to $F(t)$ of (6). The probability distribution $\Pi_2(t,\omega)$ will consist of a sum of δ functions, corresponding to configurations where there are $0,1,\ldots,n_{\max}$ DSAW's from O to M, where $n_{\max}$ is the maximum possible number of DSAW's from O to M. Clearly, there is only one configuration giving rise to $n_{\max}$ DSAW's from O to M, that is, the configuration where all the bonds are present. One sees that

$$n_{\max} = \sum_{k=0}^{t} \begin{bmatrix} k \\ t \end{bmatrix}^2 . \tag{11}$$

Let us denote by $A_{ij}(t)$ the number of configurations with j occupied bonds giving rise to i DSAW's from O to M. Since there are $2\times 2^{t(t+1)}$ bonds in total, we can write $\Pi_2(t,\omega)$ as

$$\Pi_2(t,\omega) = \sum_{i=0}^{n_{\max}} \delta(\omega - i) \times \sum_{j=0}^{2^{1+t(t+1)}} A_{ij}(t) p^j q^{(2^{1+t(t+1)}-j)} . \tag{12}$$

A table of all nonzero A_{ij} with $i \neq 0$ for $t=1-3$ is given in Appendix B. The coefficients $A_{ij}(1)$ and $A_{ij}(2)$ were also checked by hand. We did not report the $A_{ij}(4)$ and $A_{ij}(5)$ because of the large number of nonzero elements. The values of $A_{ij}(4)$ and $A_{ij}(5)$ are available upon request from the authors.

V. ANALYSIS OF THE SERIES

We used the ratio method[13] to analyze our series. First, let us examine how the series can reproduce known results. We begin by looking at $P_2(t)$.

$p > p_{cD}$. We expect $P_2(t)$ to tend to a constant for large t. Thus a plot of the quantity $\rho_t \equiv P_2(t+1)/P_2(t)$ versus $1/t$ should tend, for large t, to a horizontal straight line with ordinate at the origin equal to 1. Figure 3(a) shows such a plot and the convergence to the horizontal straight line is very fast.

$p = p_{cD}$. We expect to have $P_2(t) \sim t^{-2\beta/\nu_{\parallel}}$. A plot of $P_2(t+1)/P_2(t)$ versus $1/t$ should tend for large t toward a straight line of slope $-2\beta/\nu_{\parallel}$ and of ordinate at the origin 1. A plot of $P_2(t+1)/P_2(t)$ versus $1/t$ for $p = 0.644\,697 \simeq p_{cD}$ is shown in Fig. 3(b). Although there is a tendency toward the above trend, the series are not quite long enough to be able to retrieve the exponent $2\beta/\nu_{\parallel}$. (From Ref. 13, $2\beta/\nu_{\parallel} = 0.32 \pm 0.01$.)

$p < p_{cD}$. We expect $P_2(t) \sim \exp(-2t/\xi_{\parallel})$. A plot of $P_2(t+1)/P_2(t)$ versus $1/t$ should go toward some point

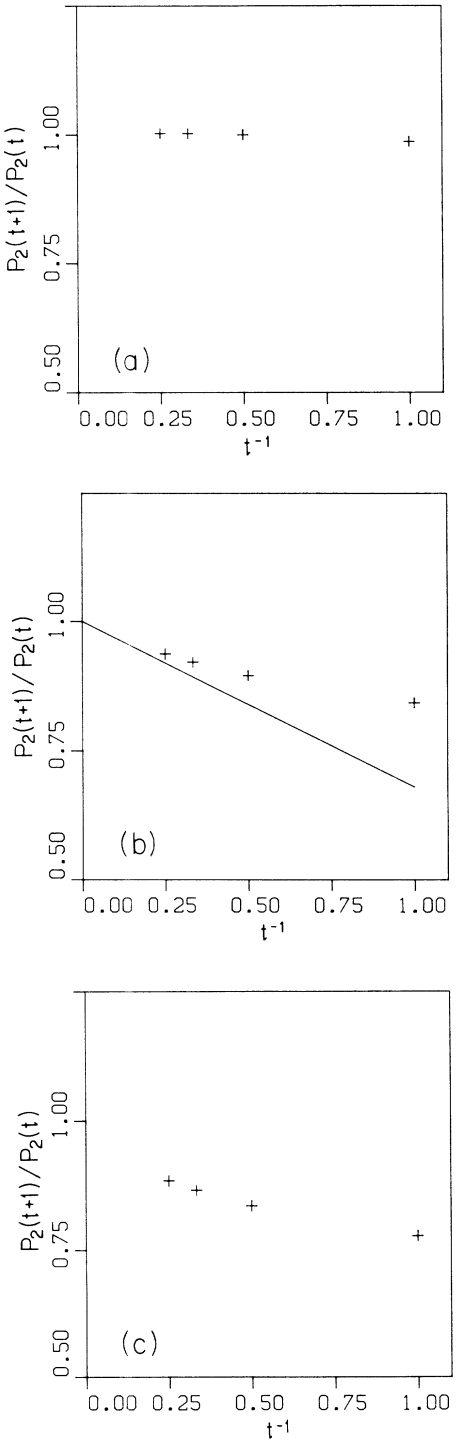

FIG. 3. Ratio plot of $P_2(t+1)/P_3(t)$ vs $1/t$ for (a) $p=0.8$, (b) $p = p_{cD} \simeq 0.644\,697$, and (c) $p=0.6$. The solid straight line in (b) has a slope of $-2\beta/\nu_{\parallel} \simeq 0.32$ and an ordinate at the origin 1.

of ordinate equal to $\exp(-2/\xi_{\parallel})$ for large t. Figure 3(c) shows $P_2(t+1)/P_2(t)$ versus $1/t$ for $p=0.6$.

Then, we look at $\langle \ln N_{\mathrm{SAW}} \rangle_{OM}$. Since for all nonzero p, $\langle \ln N_{\mathrm{SAW}} \rangle_{OM} \sim t$, we should expect the curves $\langle \ln N_{\mathrm{SAW}} \rangle_{OM}(t+1)/\langle \ln N_{\mathrm{SAW}} \rangle_{OM}(t)$ versus $1/t$ to tend, for large t, toward the straight line of slope 1 and ordinate at the origin 1. For large p, the convergence toward the asymptotic law (5) is not very good. For example, Fig. 4(a) shows $\langle \ln N_{\mathrm{SAW}} \rangle_{OM}(t+1)/\langle \ln N_{\mathrm{SAW}} \rangle_{OM}(t)$ versus $1/t$ for $p=0.8$.

At p_{cD}, the convergence is still poor. $\langle \ln N_{\mathrm{SAW}} \rangle_{OM}(t+1)/\langle \ln N_{\mathrm{SAW}} \rangle_{OM}(t)$ versus $1/t$ for $p=p_{cD}$ is shown on Fig. 4(b). Below p_{cD}, the convergence gets better and better as p is lowered. Figures

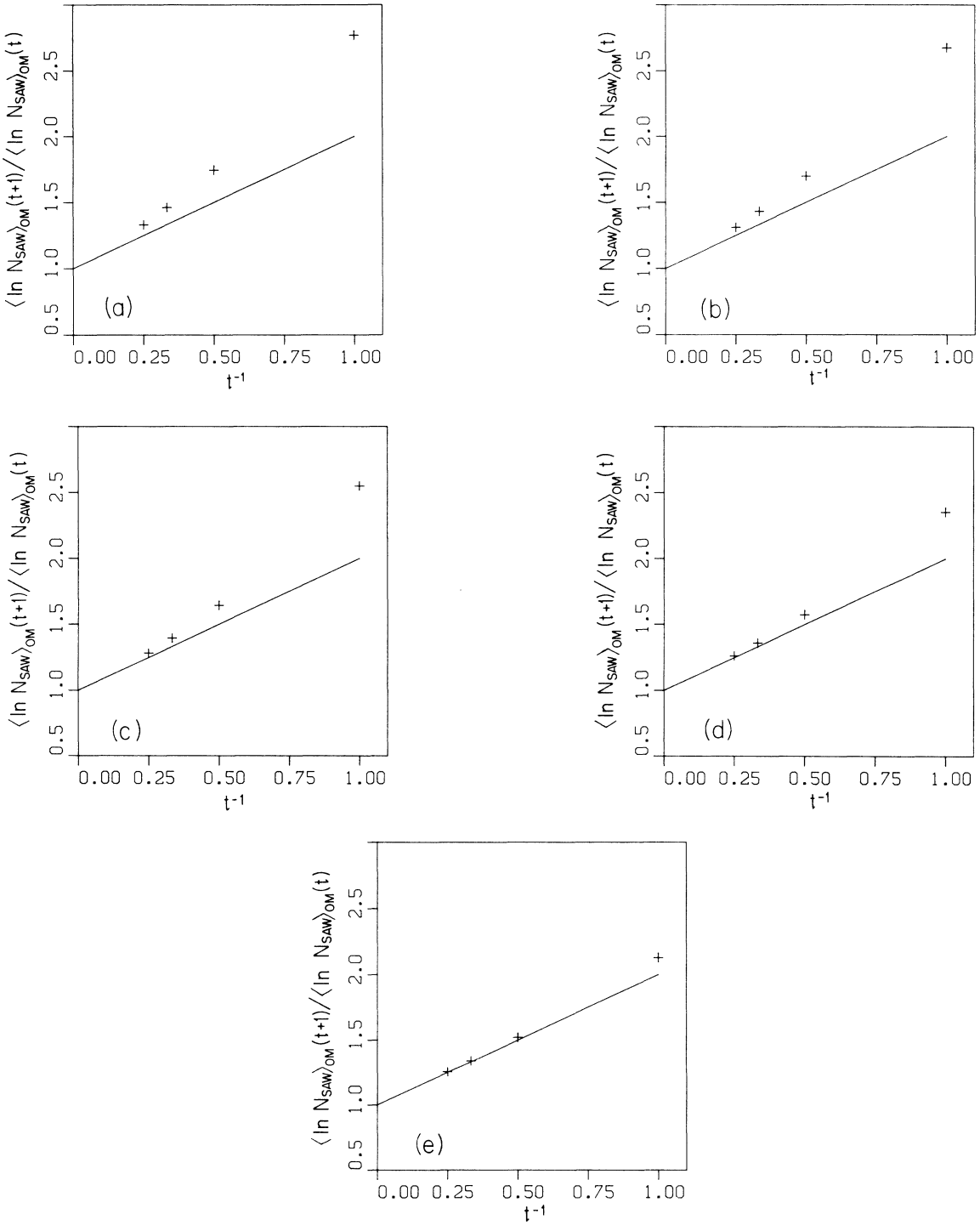

FIG. 4. Ratio plot of $\langle \ln N_{\mathrm{SAW}} \rangle_{OM}(t+1)/\langle \ln N_{\mathrm{SAW}} \rangle_{OM}(t)$ vs $1/t$ for (a) $p=0.8$, (b) $p=p_{cD}$, (c) $p=0.5$, (d) $p=0.3$, and (e) $p=0.1$. The solid straight lines have a slope of 1.

4(c)–4(e) show $\langle \ln N_{\mathrm{SAW}} \rangle_{OM}(t+1)/\langle \ln N_{\mathrm{SAW}} \rangle_{OM}(t)$ versus $1/t$ for $p=0.5$, 0.3, and 0.1, respectively.

Next, we turn to the properties of the fluctuation $F_2(t)$ of (10).

(i) *Regime 1. p close to 1.* The theory[2,6–8] predicts that

$$F_2(t) \sim t^{\zeta} , \tag{13}$$

with

$$\zeta = \tfrac{1}{3} . \tag{14}$$

However, before the true asymptotic regime is attained, there exists a regime for which

$$F_2(t) \sim t^{1/5} . \tag{15}$$

The reason is as follows. Take for simplicity the wedge geometry (see Fig. 1) and consider a particular configuration. Most of the DSAW's that can reach height t will reach it at a transverse coordinate x such that

$$-t^{1/z_{\mathrm{eff}}} \le x \le t^{1/z_{\mathrm{eff}}} , \tag{16}$$

where $1/z_{\mathrm{eff}}$ is an effective "roughening" exponent. For a pure system, $1/z_{\mathrm{eff}} = \frac{1}{2}$ and for the dilute system in the true asymptotic regime above p_{cD}, $1/z_{\mathrm{eff}} = 1/z = \frac{2}{3}$.

Consider the shaded region in Fig. 5 corresponding to $-t^{1/z_{\mathrm{eff}}} \le x \le t^{1/z_{\mathrm{eff}}}$. Let us isolate a slab of this region comprised between t and $t+dt$. Let $\exp(S_t)$ be the number of DSAW's reaching t at some x, within the shaded region. We have $\exp(S_{t+dt}) = \tau(t)\exp(S_t)$, where $\tau(t)$ is a random transmission of the slab depending on the particular configuration.

We define $T(t)$ by

$$T(t) = \ln \tau(t) . \tag{17}$$

The slab is made of different vertical elementary columns whose transmissions are independent from each other. These columns are shown in Fig. 5. The number of these columns is proportional to $t^{1/z_{\mathrm{eff}}}$. The average of $T(t)$ over the samples is a function of p. We shall denote by

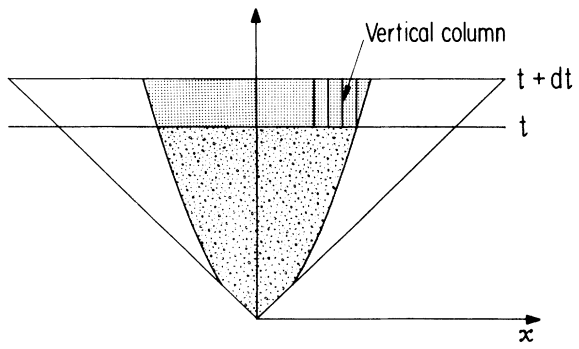

FIG. 5. The shaded area is the region of the random matrix where most of the DSAW's are located. The heavy lines are the curves $x = -t^{1/z_{\mathrm{eff}}}$ and $t^{1/z_{\mathrm{eff}}}$, which limit this region. The slab studied (see text) is the dotted region. A few vertical columns are shown.

$\langle T \rangle$ the average over samples that span. The fluctuations of T behave as

$$[\langle (T - \langle T \rangle)^2 \rangle]^{1/2} \sim t^{-1/z_{\mathrm{eff}}} . \tag{18}$$

If we neglect the correlations between the different horizontal slabs, the squared fluctuations of S take the form

$$\langle (S - \langle S \rangle)^2 \rangle = \int_a^t t^{-1/z_{\mathrm{eff}}} dt \sim t^{1-1/z_{\mathrm{eff}}} , \tag{19}$$

where a is some positive cutoff. z_{eff} is a function of t, but we have assumed that it varies slowly with time and is practically constant in the integral. S undergoes a random walk with deterministic drift in time. However, the standard deviation of the step probability decays as $t^{-1/z_{\mathrm{eff}}}$ (i.e., the walk becomes less and less random as time increases). On the other hand, there is a scaling relation relating the exponent z to the fluctuations of the free energy of the DP in a random matrix at zero temperature.[6–8,15,16] Applied to our particular case, this relation can be written as

$$2/z - \zeta = 1 . \tag{20}$$

This relation is normally valid only in the asymptotic regime. It has been explained[17] why this relation is very robust against finite-size corrections and should be satisfied even by effective exponents. It is tempting to use it also in the transient regime above. Replacing z by z_{eff} in (20) and using (19) and (13) gives

$$z_{\mathrm{eff}} = \tfrac{5}{3} \tag{21}$$

and

$$\zeta = \tfrac{1}{5} . \tag{22}$$

Figure 6(a) shows a ratio plot of $F_2(t+1)/F_2(t)$ versus $1/t$ for $p=0.99$.

(ii) *Regime 2. p larger than p_{cD} but not close to 1.* Figure 6(b) shows $F_2(t+1)/F_2(t)$ versus $1/t$ for $p=0.8$. The curve does not straighten enough as t increases in order to be able to retrieve the result $F_2(t) \sim t^{1/3}$.

(iii) *Regime 3. p close to p_{cD}.* Figure 6(c) shows $F_2(t+1)/F_2(t)$ versus $1/t$ for $p \simeq p_{cD}$. Again, the shortness of the series does not enable to draw any conclusion.

(iv) *Regime 4. $p < p_{cD}$.* Figures 6(d) and 6(e) show $F_2(t+1)/F_2(t)$ versus $1/t$ for $p=0.5$ and 0.1, respectively. For $p=0.1$, we seem to have

$$F_2(t) \sim t^{1/2} . \tag{23}$$

This result is to be compared with Ref. 1, which states that, at p_{cD},

$$\{\langle [\ln(1+N_{\mathrm{SAW}}) - \langle \ln(1+N_{\mathrm{SAW}}) \rangle_{\mathrm{span}}]^2 \rangle_{\mathrm{span}}\}^{1/2} \sim t^{1/2} . \tag{24}$$

Noting that

$$\langle \ln(1+N_{\mathrm{SAW}}) \rangle_{\mathrm{span}} = \langle \ln(N_{\mathrm{SAW}}) \rangle_{\mathrm{span}} ,$$

we expect

$$\{\langle [\ln(1+N_{\mathrm{SAW}}) - \langle \ln(1+N_{\mathrm{SAW}}) \rangle_{\mathrm{span}}]^2 \rangle_{\mathrm{span}}\}^{1/2}$$

to have the same asymptotic behavior as $F_2(t)$. On the basis of our series expansions for small p, we conjecture that, for $0 < p \leq p_{cD}$,

$$F_2(t) \sim t^{1/2} . \tag{25}$$

We now turn to the advantages of series with respect to Monte Carlo methods. One is the possibility to study quantities for small p. The other is the ability to probe quantities that are dominated by rare configurations. As noted in Ref. 1, the probability distribution of the number of DSAW's is log normal, but it has long tails. For example, if one uses the triangular geometry (Fig. 1), the average number of DSAW's, denoted by $\langle N_{\mathrm{SAW}} \rangle_{\mathrm{all}}$, is

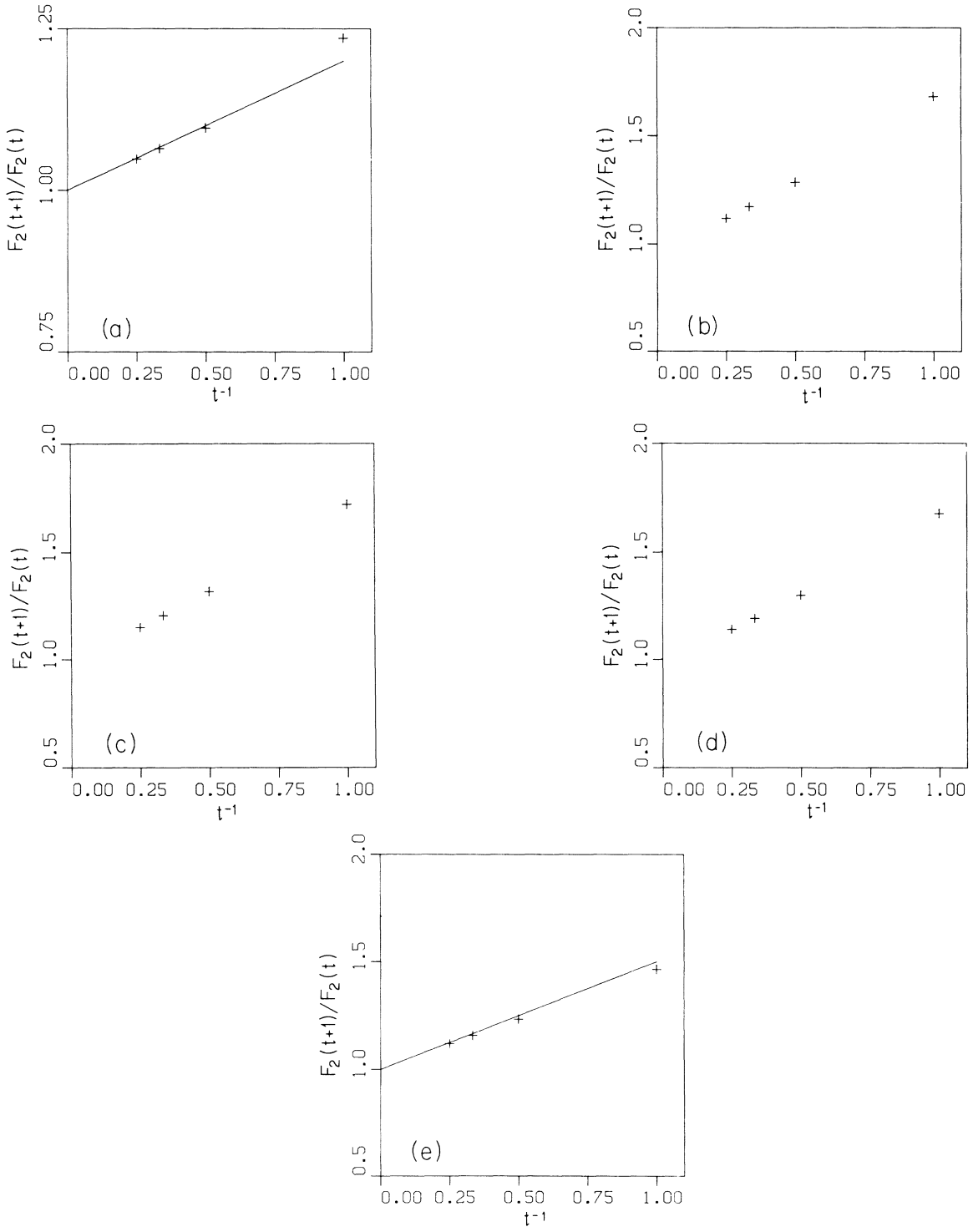

FIG. 6. Ratio plot of $\rho_t = F_2(t+1)/F_2(t)$ vs $1/t$ for (a) $p = 0.99$, (b) $p = 0.8$, (c) $p = p_{cD}$, (d) $p = 0.5$, and (e) $p = 0.1$. The solid line in (a) has a slope of $\frac{1}{5}$ and the solid line in (e) has a slope of $\frac{1}{2}$.

$$\langle N_{\mathrm{SAW}} \rangle_{\mathrm{all}} = (2p)^t . \tag{26}$$

However, $\langle \ln(1+N_{\mathrm{SAW}}) \rangle_{\mathrm{all}}$ decreases exponentially below $p_c D$, whereas $\langle N_{\mathrm{SAW}} \rangle_{\mathrm{all}}$ increases exponentially between $p=\frac{1}{2}$ and p_{cD}. This is because $\langle N_{\mathrm{SAW}} \rangle_{\mathrm{all}}$ is dominated by very rare configurations. Our series for the wedge geometry automatically reproduce the obvious result (26). With our method, one can study the averages of the moments of N_{SAW}.

VI. CONCLUSION

We have developed a new exact enumeration approach for the directed polymer in a random matrix. Even relatively short series give results consistent with what is known about percolation probabilities and exponents, and about the distribution of the number of directed self-avoided walks reaching a definite level t. The average $\langle N_{\mathrm{SAW}} \rangle$ over all configurations of the number of directed self-avoiding walks reaching level t is exactly $(2p)^t$ for the random matrix with the usual square lattice rotated by 45°, p being the bond probability. Our series automatically give this equality, whereas former Monte Carlo simulations cannot retrieve this result well below the directed percolation threshold $p_c D$. This is because N_{SAW} is dominated by rare configurations; our exact enumeration approach treats *all* configurations and hence can handle the problem of extremely rare configurations without any problem.

In the region of small probability p, we studied the rms fluctuations $F_2(t)$ of the logarithm of the number of DSAW's that reach level $2t$. We find for small p, $F_2(t) \sim t^{1/2}$ and conjecture that this behavior is valid for all $p \leq p_c D$. The averages of the moments of the numbers of DSAW's could be studied by this method.

In this paper, we restricted ourselves to the $d=2$ case. It is possible to extend the method to $d=3$, but memory storage space might become a serious problem for large t.

Note added in proof. After this work was accepted for publication, we became aware of quite recent work that is relevant.[19–21]

ACKNOWLEDGMENTS

Discussions with B. Derrida, C. Henley, N. Jan, M. Kardar, S. Redner, and Y. C. Zhang are gratefully acknowledged. The Center for Polymer Studies is supported by grants from the National Science Foundation (NSF) and U.S. Office of Naval Research (ONR). Computer time was provided by the Boston University Academic Computer Center.

APPENDIX A

In this appendix we present the method for computing the series. First, we determine $\Pi_1(t,\omega)$ for the triangular geometry up to $t=5$. Up to $t=4$, we simply enumerated all the configurations directly. We shall use an indexing of the sites of the square lattice shown in Fig. 7. A site is denoted by the couple (t,i), where the first index t is the time coordinate of this site and the second index i is its position on the x axis, starting from $i=1$ for the site which has the lowest x. The number of DSAW's starting from the origin and reaching site $(4,i)$ will be denoted by

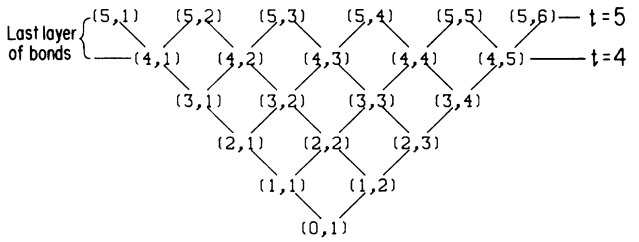

FIG. 7. Indexation of the sites of the random matrix.

$\mathcal{N}(4,i)$. Let us denote by $N_4(j_p,i_1,i_2,i_3,i_4,i_5)$ the number of configurations for a system of size $t=4$ in the triangular geometry with j_p bounds occupied, such that, for $1 \leq k \leq 5$, $\mathcal{N}(4,k)=i_k$. This means that there are $N_4(j_p,i_1,i_2,i_3,i_4,i_5)$ configurations with j_p occupied bonds, with i_1 DSAW's starting from the origin and ending at site (4,1), i_2 DSAW's to site (4,2), etc,.... .

We see that $i_1 \leq 1, i_2 \leq 4, i_3 \leq 6, i_4 \leq 4, i_5 \leq 1$. Since i_1 can be zero, $N_4(j_p,i_1,i_2,i_3,i_4,i_5)$ is a six-dimensional array of size $(20\times2\times5\times7\times5\times2)$. It has 2087 nonzero elements. The data of all i_j for $j=1$ to $t+1$ will be referred as the state of the site boundary for size t. The knowledge of this array enables the calculation of the array $N_5(j_p,i_1,i_2,i_3,i_4,i_5,i_6)$, which is the analog of $N_4(j_p,i_1,i_2,i_3,i_4,i_5)$ for level 5. Every configuration for the system of size $t=5$ can be decomposed into its part below $t=4$ and its last layer of bonds (Fig. 7). Let us consider, for example, all the configurations for a system of size $t=4$ such that $\mathcal{N}(4,1)=0$, $\mathcal{N}(4,2)=1$, $\mathcal{N}(4,3)=2$, $\mathcal{N}(4,4)=0$, and $\mathcal{N}(4,5)=0$ and such that there are j_p occupied bonds below $t=4$ (Fig. 8). If one knows the $\mathcal{N}(4,i)$, for $i=1-5$ and also the configuration of the last layer, one can readily calculate the state of the site boundary for $t=5$ [i.e., the $\mathcal{N}(5,i)$ for $i=1-6$].

Let us, for example, take the configuration of the last layer shown in Fig. 8. All the configurations for a system of size 5 that have a given state of the boundary for $t=4$ [(0,1,2,0,0) in the case of Fig. 8]; the configuration of the fifth layer shown in Fig. 8; τ occupied bonds under $t=4$ are going to have $\mathcal{N}(5,1)=0$, $\mathcal{N}(5,2)=1$, $\mathcal{N}(5,3)=3$, $\mathcal{N}(5,4)=2$, $\mathcal{N}(5,5)=0$, and $\mathcal{N}(5,6)=0$ and a total number of occupied bonds of $\tau+3$.

The weight of all these configurations is $p^{\tau}q^{20-\tau}\times N(\tau,0,1,2,0,0)\times p^4 q^6$. Thus $N_5(3+\tau,0,1,3,2,0,0)$ is incremented by $N_4(\tau,0,1,2,0,0)$. It suffices for each state of the $t=4$ boundary to enumerate the different possible configurations for the last layer in order to get $N_5(j_p,i_1,i_2,i_3,i_4,i_5,i_6)$. The algorithm actually

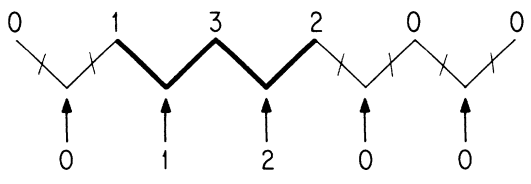

FIG. 8. A particular configuration of the last layer of bonds. Bonds which have been cut are denoted by a slash. The values of $\mathcal{N}(4,i)$ are indicated by arrows below and those of $\mathcal{N}(5,i)$ are indicated above the line $t=5$.

used is slightly more complicated. One does not need to enumerate all the different configurations for the last layer if some of the $\mathcal{N}(4,i)$, for i between 1 and 5 are zero. The method is reminiscent of the transfer matrix method of Ref. 18.

For the diamond-shaped geometry we eventually used, we must obtain the $A_{i,j}(t)$ [see Eq. (12)]. $A_{ij}(t)$ is obtained by some kind of convolution of $N_t(j_p,i_1,i_2,\cdots,i_{t+1})$ onto itself. One has

$$A_{i,j}(t)=\sum_{j,i_1,\cdots,i_{t+1},i'_1,\cdots,i'_{t+1}} N_t(j_p,i_1,i_2,\ldots,i_{t+1})N_t(j-j_p,i'_1,i'_2,\ldots,i'_{t+1})\delta(i-i_1i'_1-i_2i'_2-\cdots-i_{t+1}i'_{t+1}) . \quad (27)$$

The limitation of the procedures is not CPU time but memory space.

APPENDIX B

We give in this appendix the values of the coefficients of the series for $\Pi(\omega,t)$ [Eq. (1)]. The number of configurations with j occupied bonds giving rise to i DSAW's from O to level t will be denoted by $B_{ij}(t)$. Since there are $2^{t(t+1)}$ bonds in total, in analogy to (12), we can write

$$\Pi(\omega,t)=\sum_{i=0}^{2^{t(t+1)}}\delta(\omega-i)\sum_{j=0}^{2^{t(t+1)}}B_{ij}(t)p^jq^{2^{t(t+1)}-j} .$$

In order to display our values for the coefficients $B_{ij}(t)$, we find it more convenient to define the polynomials $\mathcal{B}_i(p,t)$ by

$$\mathcal{B}_i(p,t)=\sum_{j=1}^{2^{t(t+1)}}B_{i,j}(t)p^jq^{2^{t(t+1)}-j} .$$

$\mathcal{B}_i(p,t)$ gives the probability that the number of DSAW's reaching level t is i, when the average is done over *all* the configurations with their respective weight.

For $t=1$

$$\mathcal{B}_1(p,1)=2pq ,$$

$$\mathcal{B}_1(p,2)=p^2 ,$$

$t=2$

$$\mathcal{B}_2(p,1)=4p^4q^2+12p^3q^3+4p^2q^4 ,$$

$$\mathcal{B}_2(p,2)=2p^5q+10p^4q^2+2p^3q^3 ,$$

$$\mathcal{B}_2(p,3)=4p^5q ,$$

$$\mathcal{B}_2(p,4)=p^6 ,$$

$t=3$

$$\mathcal{B}_3(p,1)=8p^3q^9+64p^4q^8+204p^5q^7+312p^6q^6+216p^7q^5+68p^8q^4+8p^9q^3 ,$$

$$\mathcal{B}_3(p,2)=4p^4q^8+42p^5q^7+166p^6q^6+290p^7q^5+176p^8q^4+44p^9q^3+4p^{10}q^2 ,$$

$$\mathcal{B}_3(p,3)=8p^6q^6+60p^7q^5+152p^8q^4+64p^9q^3+8p^{10}q^2 ,$$

$$\mathcal{B}_3(p,4)=p^6q^6+8p^7q^5+28p^8q^4+28p^8q^4+78p^9q^3+19p^{10}q^2+2p^{11}q ,$$

$$\mathcal{B}_3(p,5)=4p^8q^4+12p^9q^3+24p^{10}q^2 ,$$

$$\mathcal{B}_3(p,6)=2p^9q^3+10p^{10}q^2+6p^{11}q ,$$

$$\mathcal{B}_3(p,7)=4p^{11}q ,$$

$$\mathcal{B}_3(p,8)=p^{12} ,$$

$t=4$

$$\mathcal{B}_4(p,1)=16p^4q^{16}+240p^5q^{15}+1632p^6q^{14}+6616p^7q^{13}+17\,636p^8q^{12}+32\,124p^9q^{11}+40\,296p^{10}q^{10}+34\,500p^{11}q^9+19\,936p^{12}q^8+7632p^{13}+q^7+1856p^{14}q^6+260p^{15}q^5+16p^{16}q^4 ,$$

$$\mathcal{B}_4(p,2)=8p^5q^{15}+144p^6q^{14}+1140p^7q^{13}+5264p^8q^{12}+15\,610p^9q^{11}+30\,686p^{10}q^{10}+39\,744p^{11}q^9+33\,010p^{12}q^8+17\,560p^{13}q^7+5984p^{14}q^6+1272p^{15}q^5+154p^{16}q^4+8p^{17}q^3 ,$$

$$\mathcal{B}_4(p,3)=16p^7q^{13}+236p^8q^{12}+1596p^9q^{11}+6188p^{10}q^{10}+14\,636p^{11}q^9+20\,680p^{12}q^8+15\,976p^{13}q^7+6996p^{14}q^6+1780p^{15}q^5+252p^{16}q^4+16p^{17}q^3 ,$$

$$\mathcal{B}_4(p,4)=4p^7q^{13}+62p^8q^{12}+420p^9q^{11}+1738p^{10}q^{10}+4946p^{11}q^9+10\,002p^{12}q^8+13\,228p^{13}q^7+8623p^{14}q^6+3016p^{15}q^5+609p^{16}q^4+70p^{17}q^3+4p^{18}q^2 ,$$

$$\mathcal{B}_4(p,5)=8p^9q^{11}+108p^{10}q^{10}+640p^{11}q^9+2088p^{12}q^8+4232p^{13}q^7+5528p^{14}q^6++2612p^{15}q^5+556p^{16}q^4+52p^{17}q^3 ,$$

$$\mathcal{B}_4(p,6)=6p^9q^{11}+66p^{10}q^{10}+332p^{11}q^9+1028p^{12}q^8+2192p^{13}q^7+3144p^{14}q^6+2904p^{15}q^5+908p^{16}q^4+144p^{17}q^3+12p^{18}q^4 ,$$

$$\mathcal{B}_4(p,7)=8p^{11}q^9+96p^{12}q^8+416p^{13}q^7+976p^{14}q^6+1388p^{15}q^5+856p^{16}q^4+120p^{17}q^3+8p^{18}q^2 ,$$

$$\mathcal{B}_4(p,8)=p^{10}q^{10}+14p^{11}q^9+77p^{12}q^8+240p^{13}q^7+501p^{14}q^6+724p^{15}q^5+734p^{16}q^4+228p^{17}q^3+23p^{18}q^2+2p^{19}q ,$$

$$\mathcal{B}_4(p,9)=16p^{13}q^7+96p^{14}q^6+232p^{15}q^5+292p^{16}q^4+196p^{17}q^3+8p^{18}q^2 ,$$

$$\mathcal{B}_4(p,10)=2p^{12}q^8+16p^{13}q^7+56p^{14}q^6+124p^{15}q^5+194p^{16}q^4+150p^{17}q^3+42p^{18}q^2 ,$$

$$\mathcal{B}_4(p,11)=4p^{14}q^6+24p^{15}q^5+56p^{16}q^4+84p^{17}q^3+36p^{18}q^2 ,$$

$$\mathcal{B}_4(p,12)=p^{14}q^6+8p^{15}q^5+23p^{16}q^4+38p^{17}q^3+34p^{18}q^2+6p^{19}q ,$$

$$\mathcal{B}_4(p,13)=4p^{16}q^4+12p^{17}q^3+12p^{18}q^2+4p^{19}q ,$$

$$\mathcal{B}_4(p,14)=2p^{17}q^3+10p^{18}q^2+4p^{19}q ,$$

$$\mathcal{B}_4(p,15)=4p^{19}q ,$$

$$\mathcal{B}_4(p,16)=p^{20} .$$

Series for $t=5$ are available upon request from the authors.

APPENDIX C

In order to display our values for the coefficients $A_{ij}(t)$ [Eq. (12)], we find it more convenient to define the polynomials in the variable $p\mathcal{A}_i(p,t)$ by

$$\mathcal{A}_i(p,t)=\sum_{j=1}^{2^{1+t(t+1)}} A_{ij}(t)p^j q^{2^{1+t(t+1)}-j} .$$

$\mathcal{A}_i(p,t)$ gives the probability that the number of DSAW's reaching the uppermost point M is i, when the average is done over *all* the configurations with their respective weight.

For $t=1$

$$\mathcal{A}_1(p,1)=4p^3q+2p^2q^2 ,$$

$$\mathcal{A}_2(p,1)=p^4 ,$$

$t=2$

$$\mathcal{A}_1(p,2)=6p^{10}q^2+68p^9q^3+210p^8q^4+256p^7q^5+156p^6q^6p^5q^7+6p^4q^8 ,$$

$$\mathcal{A}_2(p,2)=20p^{10}q^2+96p^9q^3+97p^8q^4+40p^7q^5+6p^6q^6 ,$$

$$\mathcal{A}_3(p,2)=4p^{11}q+32p^{10}q^2+20p^9q^3+4p^8q^4 ,$$

$$\mathcal{A}_4(p,2)=4p^{11}q+4p^{10}q^2+4p^9q^3+p^8q^4 ,$$

$$\mathcal{A}_5(p,2)=4p^{11}q+2p^{10}q^2 ,$$

$$\mathcal{A}_6(p,2)=p^{12} ,$$

$t=3$

$$\mathcal{A}_1(p,3)=8p^{21}q^3+196p^{20}q^4+2180p^{19}q^5+13\,800p^{18}q^6+54\,940p^{17}q^7+145\,824p^{16}q^8+268\,656p^{15}q^9+354\,676p^{14}q^{10}+343\,824p^{13}q^{11}+248\,228p^{12}q^{12}+133\,836p^{11}q^{13}+53\,352p^{10}q^{14}+15\,312p^9q^{15}+3000p^8q^{16}+360p^7q^{17}+20p^6q^{18} ,$$

$$\mathcal{A}_2(p,3)=12p^{21}q^3+380p^{20}q^4+4176p^{19}q^4+23\,242p^{18}q^6+75\,104p^{17}q^7+151\,356p^{16}q^8+200\,812p^{15}q^9+183\,842p^{14}q^{10}+119\,244p^{13}q^{11}+55\,104p^{12}q^{12}+17\,844p^{11}q^{13}+3864p^{10}q^{14}+504p^9q^{15}+30p^8q^{16} ,$$

$$\mathcal{A}_3(p,4)=56p^{21}q^3+1000p^{20}q^4+7276p^{19}q^5+27\,264p^{18}q^6+57\,220p^{17}q^7+70\,956p^{16}q^8+56\,644p^{15}q^9+30\,392p^{14}q^{10}+11\,032p^{13}q^{11}+2624p^{12}q^{12}+372p^{11}q^{13}+24p^{10}q^{14} ,$$

$$\mathcal{A}_4(p,4)=6p^{22}q^2+132p^{21}q^3+1404p^{20}q^4+7268p^{19}q^5+19\,824p^{18}q^6+29\,920p^{17}q^7+30\,887p^{16}q^8+23\,180p^{15}q^9+12\,602p^{14}q^{10}+4800p^{13}q^{11}+1208p^{12}q^{12}+180p^{11}q^{13}+12p^{10}q^{14} ,$$

$$\mathcal{A}_5(p,4)=124p^{21}q^3+1324p^{20}q^4+5668p^{19}q^5+10\,578p^{18}q^6+11\,804p^{17}q^7+8278p^{16}q^8+3712p^{15}q^9+1042p^{14}q^9+168p^{13}q^{11}+12p^{12}q^{12} ,$$

$$\mathcal{A}_6(p,4)=10p^{22}q^2+216p^{21}q^3+1644p^{20}q^4+5044p^{19}q^5+8238p^{18}q^6+8700p^{17}q^7+6208p^{16}q^8+2952p^{15}q^9+894p^{14}q^{10}+156p^{13}q^{11}+12p^{12}q^{12} ,$$

$$\mathcal{A}_7(p,4)=24p^{22}q^2+308p^{21}q^3+1534p^{20}q^4+2904p^{19}q^5+2928p^{18}q^6+1684p^{17}q^7+564p^{16}q^8+104p^{15}q^9+8p^{14}q^{10} ,$$

$$\mathcal{A}_8(p,4)=14p^{22}q^2+200p^{21}q^3+795p^{20}q^4+1392p^{19}q^5+1586p^{18}q^6$$
$$+1200p^{17}q^7+623p^{16}q^8+236p^{15}q^9+66p^{14}q^{10}+12p^{13}q^{11}+p^{12}q^{12} ,$$
$$\mathcal{A}_9(p,4)=16p^{22}q^2+272p^{21}q^3+802p^{20}q^4+968p^{19}q^5+652p^{18}q^6$$
$$+296p^{17}q^7+96p^{16}q^8+20p^{15}q^9+2p^{14}q^{10} ,$$
$$\mathcal{A}_{10}(p,4)=4p^{23}q+52p^{22}q^2+284p^{21}q^3+451p^{20}q^4+596p^{19}q^5+598p^{18}q^6$$
$$+404p^{17}q^7+170p^{16}q^8+40p^{15}q^9+4p^{14}q^{10} ,$$
$$\mathcal{A}_{11}(p,4)=36p^{22}q^2+96p^{21}q^3+158p^{20}q^4+128p^{19}q^5+52p^{18}q^6+8p^{17}q^7 ,$$
$$\mathcal{A}_{12}(p,4)=18p^{22}q^2+104p^{21}q^3+184p^{20}q^4+180p^{19}q^5+104p^{18}q^6+32p^{17}q^7+4p^{16}q^8 ,$$
$$\mathcal{A}_{13}(p,4)=44p^{22}q^2+68p^{21}q^3+86p^{20}q^4+84p^{19}q^5+50p^{18}q^6+16p^{17}q^7+2p^{16}q^8 ,$$
$$\mathcal{A}_{14}(p,4)=8p^{23}q+10p^{22}q^2+28p^{21}q^3+28p^{20}q^4+12p^{19}q^5+2p^{18}q^6 ,$$
$$\mathcal{A}_{15}(p,4)=10p^{22}q^2+44p^{21}q^3+52p^{20}q^4+24p^{19}q^5+4p^{18}q^6 ,$$
$$\mathcal{A}_{16}(p,4)=4p^{23}q+28p^{22}q^2+20p^{21}q^3+4p^{20}q^4 ,$$
$$\mathcal{A}_{17}(p,4)=4p^{23}q ,$$
$$\mathcal{A}_{18}(p,4)=4p^{22}q^2+4p^{21}q^3+p^{20}q^4 ,$$
$$\mathcal{A}_{19}(p,4)=2p^{23}q+4p^{22}q^2 ,$$
$$\mathcal{A}_{20}(p,4)=p^{24} .$$

---

[1] J. P. Nadal and J. Vannimenus, J. Phys. (Paris) **46**, 17 (1985).
[2] M. Kardar, G. Parisi, and Y. C. Zhang, Phys. Rev. Lett. **56**, 889 (1986).
[3] M. Kardar and Y. C. Zhang, Phys. Rev. Lett. **58**, 2087 (1987).
[4] B. Derrida and H. Spohn, J. Stat. Phys. **51**, 817 (1988).
[5] T. Halpin-Healy, Phys. Rev. Lett. **62**, 442 (1989).
[6] D. A. Huse, C. L. Henley, and D. S. Fisher, Phys. Rev. Lett. **55**, 2924 (1985).
[7] D. A. Huse and C. L. Henley, Phys. Rev. Lett. **54**, 2708 (1985).
[8] M. Kardar, Phys. Rev. Lett. **55**, 2923 (1985).
[9] A. J. Mac-Kane and M. A.. Moore, Phys. Rev. Lett. **60**, 527 (1988).
[10] E. Medina, T. Hwa, M. Kardar, and Y. C. Zhang, Phys. Rev. A **39**, 3053 (1989).
[11] D. Forster, D. R. Nelson, and M. J. Stephen, Phys. Rev. A **16**, 732 (1977).
[12] S. Zalesky, Physica D **34**, 427 (1989).
[13] W. Kinzel, in *Percolation Structures and Processes,* edited by G. Deutscher, R. Zallen, and J. Adler (Hilger, Bristol, 1983).
[14] D. S. Gaunt and A. J. Guttmann, in *Phase Transitions and Critical Phenomena,* edited by C. Domb and M. S. Green (Academic, London, 1974), Vol. 5.
[15] P. Meakin, P. Ramanlal, L. M. Sander, and R. C. Ball, Phys. Rev. A **34**, 5091 (1986).
[16] J. Krug, Phys. Rev. A **36**, 5465 (1987).
[17] D. E. Wolf and J. Kertész, Phys. Rev. Lett. **63**, 1191 (1989).
[18] J. Blease, J. Phys. C **10**, 3461 (1977).
[19] J. Cook and B. Derrida, Europhys. Lett. **10**, 195 (1989); J. Phys. A (to be published).
[20] B. Derrida and O. Golinelli (unpublished).
[21] W. Renz (unpublished).

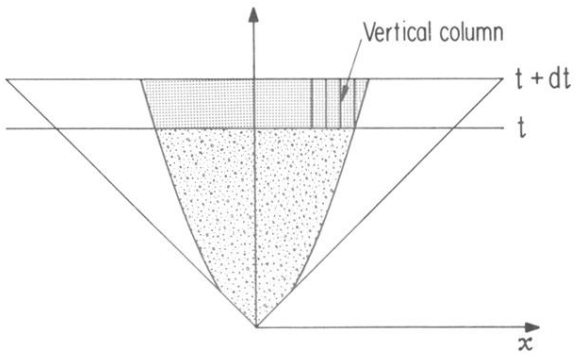

FIG. 5. The shaded area is the region of the random matrix where most of the DSAW's are located. The heavy lines are the curves $x = -t^{1/z_{\text{eff}}}$ and $t^{1/z_{\text{eff}}}$, which limit this region. The slab studied (see text) is the dotted region. A few vertical columns are shown.